**Indonesian Journal of Electrical Engineering and Computer Science**
Vol. 38, No. 2, May 2025, pp. 698~712
ISSN: 2502-4752, DOI: 10.11591/ijeecs.v38.i2.pp698-712 

# Temperature-dependent based optimal reactive power dispatch by chaotic equilibrium optimization algorithm

**Minh Trung Dao[1,2], Ngoc Dieu Vo[1,3]**
[1]Department of Power Systems, Faculty of Electrical and Electronics Engineering, Ho Chi Minh City University of Technology (HCMUT), Ho Chi Minh City, Vietnam
[2]Department of Electrical Engineering, College of Engineering Technology, Can Tho University, Can Tho City, Vietnam
[3]Vietnam National University Ho Chi Minh, Linh Trung Ward, Thu Duc City, Ho Chi Minh City, Vietnam

**Article Info**

***Article history:***

Received Mar 28, 2024
Revised Oct 29, 2024
Accepted Nov 11, 2024

***Keywords:***

Equilibrium optimization
Optimal reactive power dispatch
Power loss
Temperature effect
Voltage deviation

**ABSTRACT**

The optimal reactive power dispatch (ORPD) problem is considered as an important aspect in power system operation of the reactive power, which is vital to maintain network voltage within desirable limit for system reliability. In conventional ORPD problem, the resistance of components in power systems is considered to be independent to their temperature variations. Actually, there is a correlation between the branch resistance and temperature, thus the temperature should be taken into account when performing power flow analysis to improve the accuracy in the calculation of the power flow and power loss on branches. This paper proposes a new chaotic equilibrium optimization (CEO) method to solve the temperature-dependent based optimal reactive power dispatch (TDORPD) problem in power systems by optimizing the reactive power loss and voltage deviation. The proposed CEO algorithm is implemented for the conventional ORPD and TDORPD problems on the benchmark IEEE 30 bus testing network. Moreover, the effects of temperature variations on the considered TDORPD problem are also considered. The obtained results have demonstrated a better performance of the proposed CEO algorithm compared to the original EO and other methods in the literature review for the problem in terms of the solution quality, which confirms its efficacy to effectively resolve the ORPD and TDORPD problem.



***Corresponding Author:***

Ngoc Dieu Vo
Department of Power Systems, Faculty of Electrical and Electronics Engineering
Ho Chi Minh City University of Technology (HCMUT)
268 Ly Thuong Kiet Street, District 10, Ho Chi Minh City, Vietnam
Email: vndieu@hcmut.edu.vn

## 1. INTRODUCTION

An accurate analysis of power flow always plays a pivotal role in the scheduling, operation, and expansion of power system, addressing issues such as contingency analysis, transient stability, and economic dispatch. Hence, the precise power flow calculation in power system is imperative. In power system, every equipment has interior resistance which varies with temperature, particularly evident in overhead lines where current flow induces joule losses, increasing line temperature. For instances, environmental factors, conductor diameter, and emissivity influence line temperature. Although resistance for pure conductors is a function of temperature growth, conventional power studies completely ignore the temperature effect. Additionally, the assumption of constant line resistance in typical power flow studies comes up to temperature-induced errors in power flow as well as the computations of power loss in branches.

Temperature rise must be considered in the computation in order to get precise branch losses. Optimal power flow has been recognized as a crucial instrument in evaluating the financial performance of the electricity market in a deregulated electricity framework. Therefore, temperature effect has a big impact on power flow accuracy [1].

The optimal reactive power dispatch (ORPD) stands as a pivotal optimization challenge crucial for ensuring the safeness and stable operation of power systems. Within the ORPD framework, the primary aim is minimizing the active power loss in power systems subject unit and system constraints. To achieve this objective, control variables including voltage at generation buses, reactive power shunt compensations, and power transformer taps are optimized by the ORPD problem. Therefore, it is essential to adhere to constraints concerning the power balance at buses, generator output limits, and security limits, rendering the ORPD problem a difficult and expansive optimization problem. Traditionally, the ORPD problem in power systems has garnered significant attention across various applications, employing both classical and cutting-edge optimization methodologies. On that account, a fully coupled temperature-dependent power flow approach is adopted in this study as well as the effects of temperature variations on the considered TDORPD problem.

To solve the ORPD problem, some traditional optimizers have been proposed, including the interior point method [2]-[3], linear programming [3], quadratic programming [4], Newton method [5], and nonlinear programming [6], gradient search [7], dynamic programming method [8], and Lagrangian method [9]. As could be seen clearly, these methods have achieved optimal results with reasonable quality. However, they have suffered from some drawbacks for dealing with the practical ORPD problem. For instances, the Interior Point Method frequently suffers with sophisticated implementation and is extremely sensitive to starting points, rendering it ineffective for large-scale tasks [2]-[3]. Linear Programming is confined to linear issues and may produce approximation mistakes when applied to nonlinear systems [3]. Similarly, quadratic programming is limited to quadratic objectives, making it difficult to deal with non-linearity [4]. The Newton Method is fast but necessitates computationally costly Hessian matrices, and can be sensitive to initial assumptions, with a preference for local convergence [5]. Nonlinear programming incurs substantial computational costs and is prone to and ended up stick in local optima, resulting in sluggish convergence [6]. Gradient-based approaches, while commonly used, are prone to local minima and rely heavily on step size and differentiability [7]. Dynamic programming suffers not only from dimensionality but also resulting in excessive memory utilization and difficult formulas [8]. Finally, the Lagrangian Method frequently faces non-convex issues, where duality gaps and parameter tuning difficulties might limit its usefulness [9].

In the last two decades, metaheuristic algorithms have recently been demonstrated to be capable of finding optima or near-optima solutions to a various optimization problems in a variety of engineering disciplines. The following are some prominent studies that have applied metaheuristic methods to ORPD problems: moth-flame optimization (MFO) [10], water cycle algorithm (WCA) [11], gravitational search optimization (GSO) [12], teaching-learning-based optimization (TLBO) [13], differential evolution optimization (DEO) [14], exchange market algorithm (EMA) [15], genetic algorithm (GA) [16], particle swarm optimization (PSO) [17], [18], artificial bee colony optimization (ABCO), differential search algorithm (DSA) [19], krill herd algorithm (KHA) [20], gray wolf optimization (GWO) [21], ant lion optimization (ALO) [22], [23], whale optimizer algorithm (WOA) [24]-[26], backtracking search (BSA) [27], stochastic fractal search (SFS) [28], social spider algorithm (SSA) [29], and archimedes optimization (AO) [30]. Despite the fact that such the methods have demonstrated the satisfactory performance and accuracy increment when solving the ORPD problem, they remain reliant on the conventional power flow problem for their calculations. In order to enhance the precision of the ORPD solution, it is important to examine the effect of temperature in power flow computation. In ORPD, various metaheuristic algorithms struggle with notable limitations that affect their performance. MFO and PSO are susceptible to premature convergence and blocking in local optima, especially in complex high-dimensional problems [11], [12]. Similarly, WCA and ALO suffer from reduced exploration power, leading to suboptimal solutions [13], [14]. GSA and DSA often have slow convergence and poor constraint handling in ORPD [15], [16]. Algorithms such as TLBO, ABC, and GWO may exhibit limited diversity in the search process, making them susceptible to local optima [17]-[19]. DE, GA, KHA also has to due with challenges, particularly due to slow convergence and the need to carefully tune settings to balance exploration and exploitation [20]-[22]. While WOA and BSA perform well in exploration, they often exploit inefficiencies, leading to premature convergence [23], [24]. Finally, SFS and SSO struggle to remain a balance between exploration and exploitation, which affects their effectiveness in refining solutions to ORPD [25], [26].

While temperature fluctuations significantly impact load flow analysis, there remains a dearth of studies exploring their effects on power system research. Shaheen *et al.* [27] introduced the g-best guided ABC (GABC) method to tackle optimal power flow (OPF) issues considering temperature variations. Similarly, Nguyen *et al.* [28] devised a chaotic whale optimizer (CWO) for addressing the dependence of temperature in OPF problems. These investigations analyzed the temperature impact on fuel consumption,

real power losses, and resistance of components using IEEE 30 bus and 2383 bus systems. However, the existing literature lacks the exploration into the temperature effect of the ORPD issue.

Overall, the aforementioned algorithms have met several challenges such as slow convergence, sensitivity to local minima, and difficulty handling complex, nonlinear, and constrained power systems in ORPD scenarios. In addition, the existent studies neglect temperature effect on the ORPD problem. Motivated by these considerations, this research introduces a novel chaotic equilibrium optimization (CEO) method to address the dependence on temperature based optimal reactive power dispatch (TDORPD) issue in power systems. Notably, our study marks the first exploration of temperature effects on the ORPD dilemma. We enhance the CEO with a chaotic local search strategy to improve search efficiency. Implementation of the presented algorithm is executed on the IEEE 30-bus test system across multiple case studies. This paper delivers the following key contributions:

- The TDORPD is determined as the single-objective and multi-objective problems considering voltage profile enhancement and active real power loss minimization. To improve the accuracy of TDORPD problem, this study uses a fully coupled temperature-dependent power flow (FC-TDPF) approach [31] to perform power flow analysis considering the temperature effect on the components in power system.
- The chaotic methodology is amalgamated with the mature equilibrium optimizer (EO) framework to formulate a fresh metaheuristic method called CEO, specifically tailored for tackling the TDORPD conundrum. CEO is applied to address the TDORPD issue using the 30-bus network across various case studies. Different temperature increments are examined during the TDORPD problem-solving process to scrutinize their impact on the TDORPD solutions.
- The performance of the proposed CEO is evaluated and analyzed through simulation. Then, it is compared with the conventional EO method and other methods in the literature to validate its efficacy.

## 2. THE PROPOSED MOETHOD

### 2.1. The temperature-dependent power flow

The conductor resistance varies depending on the temperature of the metal conductor. As a function of temperature, resistance is given as following (1) [31]:

$$R = R_{ref} \times \frac{T+T_F}{T_{ref}+T_F} \quad (1)$$

in which, $R_{ref}$ is the resistance of branch at the reference temperature ($T_{ref}$); $R$ is the resistance of the conductor; $T$ is the temperature of the conductor; $T_F$ is the temperature coefficient.

To perform power flow analysis, this study uses a fully coupled temperature-dependent power flow approach (FC-TDPF) considering the temperature effect on the branch elements. It is assumed that the power network is operated at both a thermal and electrical steady state in the FC-TDPF. From the conventional Newton-Raphson approach, the mathematical formula of the FC-TDPF is modified in the state vector, mismatch equations, and Jacobian matrix [1].

In the FC-TDPF formulation, each temperature-dependent branch incorporates temperature $T$ as an extra state variable alongside the state variables of voltage magnitude $V$ and voltage angle $\delta$. Therefore, the considered state vector of the FC-TDPF may be expressed in per-unit as follows (2) [1]:

$$x = [V \quad \delta \quad T]^T \quad (2)$$

There are three mismatch equations in the FC-TDPF: mismatch equations for active power, reactive power, and temperature difference in the following (2)-(4) [1]:

$$\Delta P_i = (P_{Gen,i} - P_{Load,i}) - P_i(\delta, V, T) \quad (3)$$

$$\Delta Q_i = (Q_{Gen,i} - Q_{Load,i}) - Q_i(\delta, V, T) \quad (4)$$

$$\Delta H_{ij} = 0 - H_{ij}(\delta, V, T) \quad (5)$$

An additional state variable $T$ requires a reconstruction of the Jacobian matrix. Partial derivatives of active power, reactive power, and temperature difference equations are determined according to ($V$, $\delta$. and $T$). The modified Jacobian matrix is defined as follows (6), (7) [1]:

$$J(\delta,V,T)=\begin{bmatrix}\frac{\partial P}{\partial \delta} & \frac{\partial P}{\partial V} & \frac{\partial P}{\partial T}\\ \frac{\partial Q}{\partial \delta} & \frac{\partial Q}{\partial V} & \frac{\partial Q}{\partial T}\\ \frac{\partial H}{\partial \delta} & \frac{\partial H}{\partial V} & \frac{\partial H}{\partial T}\end{bmatrix} \quad (6)$$

$$\begin{bmatrix}\delta^{v+1}\\ V^{v+1}\\ T^{v+1}\end{bmatrix}=\begin{bmatrix}\delta^{v}\\ V^{v}\\ T^{v}\end{bmatrix}-J(\delta^{v},V^{v},T^{v})^{-1}\cdot\begin{bmatrix}\Delta P^{v}\\ \Delta Q^{v}\\ \Delta H^{v}\end{bmatrix} \quad (7)$$

The main process for solving the FC-TDPF problem can be expressed in the following steps [31]:

- Initialize all the state variables (magnitude $V$, $\delta$. and $T$);
- Modify the resistances of all branches to match the most recent temperature estimate, as given in (1);
- Update the admittance matrix $Y_{bus}$ using the values of branch resistances;
- Formulate the modified Jacobian matrix based on (6);
- Define the mismatch of three equations based on (3), (4), and (5);
- Define the updated in (7):
- Performed the loop repeatedly until the three mismatches ($\Delta P$, $\Delta Q$, $\Delta H$) are within the range of tolerances desired.

### 2.2. Problem formulation

The priority achievement of the temperature-dependent based optimal reactive power dispatch (TDORPD) problem aims to minimize predefined objective functions while assuring system constraints. The TDORPD formulation considers two objectives: active power loss and voltage deviation. Furthermore, all the constraints of the transmission network must be satisfied by the TDORPD solution, including real and reactive power balance, generator outputs limits, and other constraints of shunt compensation, load bus voltage, and power flow limits on transmission lines. Hence, the TDORPD problem includes control variables (vector $u$) and state variables (vector $x$), which can be described as follows (8), (9):

$$u=[V_{G1},\dots,V_{G,NG},Q_{C1},\dots,Q_{C,NC},T_1,\dots,T_{NT}]^T \quad (8)$$

$$x=[V_{L1},\dots,V_{L,ND},Q_{G1},\dots,Q_{G,NG},S_{L1},\dots,S_{L,NL}]^T \quad (9)$$

where, $V_G$ represents the generator bus voltage; $Q_C$ signifies the reactive power output of shunt compensation; $T$ signifies the transformer tap; $V_L$ signifies the load bus voltage; $Q_G$ signifies the reactive power generation; $S_L$ signifies the apparent power flow on transmission lines; *NG* indicates the number of generation buses; *NC* indicates the number of shunt capacitors; *NT* indicates the number of transformers with on load tap changer; *ND* indicates the number of load buses; *NL* indicates the number of branches.

#### 2.2.1. Objective functions

a. Case 1: minimization of real power loss

The TDORPD aims to minimize the active power loss of the transmission system as following (10) [32]:

$$P_L=\sum_{q=1}^{NL}G_{q(ij)}\left[V_i^2+V_j^2-2V_iV_j\,cos(\delta_i-\delta_j)\right] \quad (10)$$

where, $G_{q(ij)}$ symbolizes the transfer conductance of $q$ branch between bus $i$ and bus $j$; the voltage magnitude and voltage angle at the bus $i$ are represented by $V_i$ and $\delta_i$, respectively.

b. Case 2: Minimization of voltage profile

The aim of voltage deviation (VD) minimization indicates the voltage deviation improvement at all load buses in the system from the nominated value 1.0 p.u.. The value of VD can be represented in the follows (11) [32]:

$$VD=\sum_{i=1}^{ND}\left|V_{L_i}-1\right| \quad (11)$$

c. Case 3: Minimization of real power loss and voltage deviation

The objective functions of active power loss and *VD* are computed simultaneously in the multi-objective optimization of TDORPD as following (12):

$$f(x,u)=\lambda_1P_L+\lambda_2VD \quad (12)$$

where, $P_L$ and $VD$ are defined according to (10) and (11), respectively. $\lambda_1$ and $\lambda_2$ are selected as 1 and 10, respectively.

### 2.2.2. Constraints

a. Power and heat balance constraints

The balance constraints represent typical nonlinear power flow equations as following (13)-(15):

$$P_{Gi} - P_{Di} = V_i \sum_{j=1}^{NB} V_j \left[ G_{ij}\, cos(\delta_i - \delta_j) + jB_{ij}\, sin(\delta_i - \delta_j) \right]; i = 1, \ldots, n \quad (13)$$

$$Q_{Gi} - Q_{Di} = V_i \sum_{j=1}^{NB} V_j \left[ G_{ij}\, sin(\delta_i - \delta_j) - jB_{ij}\, cos(\delta_i - \delta_j) \right]; i = 1, \ldots, n \quad (14)$$

$$T_{ij} - \left[ T_{Amp} + R_{\theta,ij} \left( g_{ij}(T) \times (V_i^2 + V_j^2) - 2g_{ij}(T) \times V_i V_j\, cos(\delta_i - \delta_j) \right) \right]; i = 1, \ldots, NB \quad (15)$$

where, $NB$ is the number of buses; $G_{ij}$ and $B_{ij}$ are the transfer of conductance and susceptance between buses $i$ and $j$, respectively; $P_{D,i}$ is the active while $Q_{D,i}$ is the reactive at load buses.

b. Limit constraints

Generator power and voltage constraints: The real power, reactive power, and voltage limits of the generators are represented by the inequality (16)-(18) as follows:

$$P_{Gk}^{min_{Gk} max_{Gk}} \quad (16)$$

$$Q_{Gk}^{min_{Gk} max_{Gk}} \quad (17)$$

$$V_{Gk}^{min_{Gk} max_{Gk}} \quad (18)$$

Transformer tap constraint: The limits of transformer taps are represented by the following inequality (19):

$$T \quad m_{min_m}^{m=1,\ldots,NT\ max_m} \quad (19)$$

Shunt reactive power compensation constraint: The limits of shunt compensation of reactive power sources are represented by the following inequality (20):

$$Q \quad Ci_{min_{Ci}}^{i=1,\ldots,NC\ max_{Ci}} \quad (20)$$

Load bus voltage and branch's power flow constraints: The voltage at load buses and power flow on transmission lines are represented by the inequality as follows (21), (22):

$$V \quad Li_{min_{Li}}^{i=1,\ldots,ND\ max_{Li}} \quad (21)$$

$$S_{Li} \leq S_{Li}^{max} \quad i = 1, \ldots, NL \quad (22)$$

It is necessary to impose inequality constraints on a fitness function as quadratic penalty terms as shown (23):

$$Fit = f(u,x) + \lambda_Q \sum_{i=1}^{NG\sum V} \sum_{i=1}^{ND\sum S} \sum_{i=1}^{NL\sum (S_{Li} - S_{Li}^{max^2}} (V_{Li} - V_{Li}^{lim^2} (Q_{Gi} - Q_{Gi}^{lim^2} \quad (23)$$

in which, $\lambda_V$, $\lambda_Q$, and $\lambda_S$ are penalty factors, $x^{\text{lim}}$ denotes the limit values of the dependent variables $x$, which can be described by the following expression:

$$x^{lim} \begin{cases} x_{max} & \text{if } x > x_{max} \\ x_{min} & \text{if } x < x_{min} \end{cases} \quad (24)$$

## 2.3. Chaotic equilibrium optimization

### 2.3.1. Conventional EO algorithm

Due to a controlled volume, with the inspiration of the dynamic equilibrium of mass, a recent optimization technique known as equilibrium optimization (EO) has emerged [33]. The EO method employs

a collection of particles, where the result to the optimization problem under consideration is depicted by the positions of these particles, which are also called concentrations. In the EO, the average of four optimal solutions are chosen to establish the equilibrium pool. During the process for optimization, the particles' positions are continuously adjusted based on randomly selected equilibrium candidates from the equilibrium pool to achieve the equilibrium.

Firstly, EO creates a population of *N* particles from the search space as following (25):

$$C_{i,initial} = C_{min} + rand_i(C_{max} - C_{min}), i = 1,2,\dots,N \quad (25)$$

in which, *N* is the size of population; $C_{i,initial}$ is the vector of initial concentration for particle *i*; $rand_i$ is a random number in the range [0, 1]; $C_{\max}$ and $C_{\min}$ are the upper and lower boundaries for each dimension of the considered problem, respectively.

After the population is initialized, each particle's performance is assessed by evaluating the objective function. For instances, GWO utilizes three best-so-far candidates, such as alpha, beta, and gamma wolves, to update the positions of the other wolves. Nevertheless, using less than four candidates degrades the performance of the method in multimodal and composition functions but will enhance the results in unimodal functions [34]. In term of EO, it designates the top solutions as equilibrium candidates due the particles, which are ordered based on their fitness function values. Along with their average solution, the EO method then creates the equilibrium pool by choosing the four best candidate concentrations as follows (26), (27):

$$C_{eq,pool} = [C_{eq1}, C_{eq2}, C_{eq3}, C_{eq4}, C_{eq,ave}] \quad (26)$$

where:

$$C_{eq\_ave} = \frac{C_{eq1}+C_{eq2}+C_{eq3}+C_{eq4}}{4} \quad (27)$$

The position of each particle can be modified by randomly selecting among the five equilibrium candidates. Thus, the updating operator for updating the position of particles is represented by [33]:

$$C_i^{iter+1} = C_{eq} + (C_i^{iter} - C_{eq})F + \frac{G}{\lambda V}(1 - F) \quad (28)$$

where, $C_i^{iter}$ and $C_i^{iter+1}$ are the concentration vectors of particle *i* at iterations *iter* and (*iter*+ 1), respectively; $C_{eq}$ is a vector of equilibrium concentration which randomly selected from the equilibrium pool; *F* is the exponential term; *G* is the generation rate; *V* value is set to 1; $\lambda$ is a random vector in the range [0,1].

In (28), the component *F* which is an exponential one serves to balance exploitation and exploration in EO, as demonstrated:

$$F = a_1 sign(r_1 - 0.5)(e^{-\lambda t} - 1) \quad (29)$$

where, $a_1$ is a constant ($a_1$ = 2), $r_1$ is a random number from 0 to 1; *t* represents the linearly reduced nonlinear factor described by:

$$t = \left(1 - \frac{iter}{iter_{max}}()^{\left(a_2 \frac{iter}{iter_{max}}()\right)}\right) \quad (30)$$

where, $a_2$ is a constant ($a_2$ = 1); $iter_{\max}$ is the maximum iterations.

The generation term *G* which can be applied to improve the exploitation capability of the EO is represented as following (31), (32):

$$G = GCP(C_{eq} - \lambda C)F \quad (31)$$

where:

$$GCP = \begin{cases} 0.5r_1 & r_2 \geq GP \\ 0 & \text{otherwise} \end{cases} \quad (32)$$

in which, *GCP* represents a vector of control parameters for the generations; the value of *GP* is set to 0.5.

### 2.3.2. Proposed CEO algorithm

In the proposed CEO method, the conventional EO is augmented with a chaotic local search (CLS) to enhance the search capability CEO. Two optimization phases are integrated in the proposed CEO. In the number one phase, the conventional EO method was employed to adjust particles within the populations in the considered domain. During the number two phase, the CLS approach is utilized to explore the vicinity of the current most optimal solution to identify an improved solution [35]. A new solution is generated according to the current best solution using CLS, as depicted in the following equation:

$$X_{best,k}^{new} = X_{best,k} + (Z_k - 0.5) \times (X_{i,k} - X_{j,k}) \quad (33)$$

where, $X_{best,k}^{new}$ and $X_{best,k}$ are the new best and current best position solutions which are generated from the CLS at iteration $k$; $X_{i,k}$ and $X_{j,k}$ are the two solutions which are randomly chosen among the individuals in the current population.

This new obtained best solution is used to replace the current best one from the current population if the fitness function value of this solution is better than the current best one. The term $Z_k$ in (33) is a chaotic sequence variable generated by using the logistic map as follows:

$$Z_{k+1} = \mu \times Z_k \times (1 - Z_k) \quad (34)$$

in which, $Z_k \in (0,1)\ \forall k \in \{0,1,2,\dots\}$ and $\mu \in (0,4)$.

### 2.3.3. Implementation of the proposed CEO to the TDOPF problem

The overall procedure for applying the proposed CEO method for solving the TDORPD problem includes the main steps as follows:

- Specify the power system data, objective functions, boundaries for control variables, as well as all the set constraints of the problem.
- Set control parameters for CEO including $N$, $GP$, $a_1$, $a_2$, $K$, and $Iter_{\max}$.
- Randomly initialize a population according to the formula provided in (25).
- Solve the FC-TDPF problem and calculate the fitness function value for each particle in the initial population using (23). Set the begin number of iterations $Iter = 0$.
- Increase the number of iterations $Iter = Iter + 1$ and then select the four best particles including $C_{eq1}$, $C_{eq2}$, $C_{eq3}$, and $C_{eq4}$ with the lowest fitness value to calculate the average particle ($C_{eq,ave}$) using (27).
- Use (26) to create the equilibrium pool $C_{eq,pool}$.
- If $Iter > 1$, perform the memory saving.
- Randomly choose a candidate from the obtained equilibrium pool ($C_{eq,pool}$). Use (29), (31), and (32) to generate the $F$, $G$, and $GCP$ vectors respectively.
- Use (28) to update the concentration of the particle $C_i$.
- Apply (33) to perform the CLS approach.
- If $Iter <= Iter_{\max}$, return to Step 5; Otherwise, stop the iteration process.

## 3. SIMULATION RESULTS

The proposed method is developed in this study to resolve the conventional ORPD and TDORPD model on the IEEE 30-bus network. According to Figure 1, this system consists of six generators, 41 branches, four transformers, and nine shunt compensators. The load demands of active power is 283.4 MW while reactive power is 126.2 MVA. The detail of this system can be found in [6]. This test network includes 19 control variables. The proposed CEO method is programmed by MATLAB R2021b platform. The CEO's control parameters are configured as follows: $N = 50$, $a_1 = 2$, and $a_2 = 1$, $GP = 0.5$, $K = 10$, $Iter_{max} = 600$. Additionally, the CEO undergoes 10 independent trials for each test case. The conventional EO method is evaluated for comparison purposes. Furthermore, power flow computations are performed using the FC-TDPF toolbox [1].

### 3.1. The conventional ORPD problem

In this first case, Case 1 represent for the single-objective of active power loss, Case 2 represent for the single-objective of voltage deviation while Case 3 represents for the multi-objective of active power loss and voltage deviation.

### 3.1.1. The case of single-objective function

To study the efficacy of the suggested CEO, it is used to the conventional ORPD problem. The objective functions of active power loss ($P_L$) and voltage deviation (*VD*) are considered individually in Cases 1 and 2, respectively. Table 1 records the optimal results including the optimal set of control variables yielded by the suggested CEO and EO methods for the 30-bus network. Moreover, obtained results for state variables, such as load bus voltages and reactive power outputs of generators of ORPD solution obtained by CEO are given in Table 1 and Figure 2.

From Table 1 and Figure 2, all state variables are kept within their acceptable limitations. Table 2 provides a results comparison obtained by the proposed CEO method and other algorithms. In Case 1, the best active power loss prevailed by the proposed CEO method (8.123 MW) is comparable to SHADE-SF and is better than that of other methods such as MFO, NGBWCA, QOTLBO, IGSA-CSS, EMA, FAHCLPSO, DE, OGSA, and HFA.

From Table 2, it may also find that the proposed CEO method also performed better than MFO, IGSA-CSS, and HFA for minimizing the voltage deviation in Case 2. Figure 3 and Figure 4 show fitness values over 600 iterations for Cases 1 and 2, respectively, which presents the proposed EO and CEO convergence characteristics. These figures show that the suggested CEO converges promptly towards the near-optimal solutions and obtains better values of active power loss and *VD* compared with EO method.

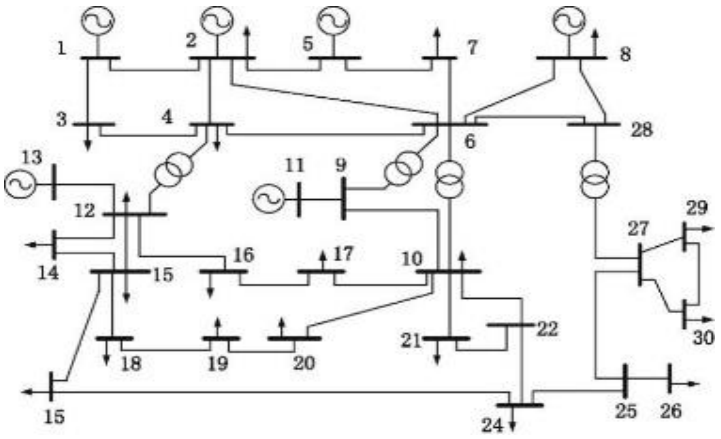


Figure 1. The IEEE 30-bus network

Table 1. Optimal results for Cases 1, 2, and 3 of conventional ORPD problem

| Parameters | Case 1 | | Case 2 | | Case 3 | |
|---|---|---|---|---|---|---|
| | CEO | EO | CEO | EO | CEO | EO |
| $V_{G1}$ (pu) | 1.0689 | 1.0668 | 1.0016 | 1.0207 | 1.0259 | 1.0273 |
| $V_{G2}$ (pu) | 1.0601 | 1.0584 | 0.9983 | 1.0222 | 1.0182 | 1.0196 |
| $V_{G5}$ (pu) | 1.0368 | 1.0352 | 1.0175 | 1.0194 | 1.0009 | 1.0028 |
| $V_{G8}$ (pu) | 1.0424 | 1.0416 | 1.0076 | 1.0059 | 1.0020 | 1.0047 |
| $V_{G11}$ (pu) | 1.0889 | 1.0650 | 1.0531 | 1.0091 | 1.0745 | 1.0147 |
| $V_{G13}$ (pu) | 1.0502 | 1.0618 | 1.0210 | 0.9937 | 0.9885 | 1.0070 |
| $Q_{C10}$ (MVar) | 1.0528 | 1.0324 | 1.0725 | 1.0222 | 1.0971 | 1.0288 |
| $Q_{C12}$ (MVar) | 0.9273 | 0.9457 | 0.9000 | 0.9000 | 0.9000 | 0.9000 |
| $Q_{C15}$ (MVar) | 0.9888 | 1.0039 | 0.9984 | 0.9538 | 0.9542 | 0.9764 |
| $Q_{C17}$ (MVar) | 0.9765 | 0.9762 | 0.9664 | 0.9673 | 0.9647 | 0.9649 |
| $Q_{C20}$ (MVar) | 0.3212 | 4.9999 | 4.9958 | 5.0000 | 5.0000 | 4.9986 |
| $Q_{C21}$ (MVar) | 4.4130 | 0.4523 | 0.3609 | 1.5054 | 4.9803 | 0.0942 |
| $Q_{C23}$ (MVar) | 3.8925 | 4.9989 | 4.9999 | 5.0000 | 5.0000 | 5.0000 |
| $Q_{C24}$ (MVar) | 4.9890 | 5.0000 | 0.0001 | 0.0470 | 0.0002 | 1.1707 |
| $Q_{C29}$ (MVar) | 3.8742 | 3.5204 | 4.9997 | 5.0000 | 5.0000 | 4.9997 |
| $T_{11}$ (pu) | 5.0000 | 4.9992 | 4.9999 | 4.9975 | 4.9973 | 5.0000 |
| $T_{12}$ (pu) | 3.0347 | 4.9824 | 4.9998 | 4.9997 | 5.0000 | 4.9994 |
| $T_{15}$ (pu) | 4.9982 | 4.9995 | 4.9998 | 5.0000 | 4.9886 | 4.9990 |
| $T_{36}$ (pu) | 2.4383 | 2.3766 | 2.5540 | 3.1611 | 2.5258 | 2.6341 |
| Power loss (MW) | 4.4107 | 4.4197 | 5.4939 | 5.1544 | 4.8779 | 4.8777 |
| *VD* (pu) | 0.9026 | 0.9139 | 0.0874 | 0.0915 | 0.0998 | 0.1038 |
| Fitness function | 4.4107 | 4.4197 | 0.0874 | 0.0915 | 5.8764 | 5.9152 |

Table 2. Result comparisons for cases 1, 2, and 3 of conventional ORPD problem

| Case | Method | Active power loss (MW) | *VD* (pu) |
|---|---|---|---|
| 1 | CEO | 4.4107 | 0.9026 |
| | EO | 4.4197 | 0.9139 |
| | MFO [10] | 4.5128 | - |
| | NGBWCA [11] | 4.4801 | 0.8413 |
| | QOTLBO [13] | 4.5594 | 1.9057 |
| | IGSA-CSS [12] | 4.7660 | - |
| | EMA [15] | 4.4978 | 0.8123 |
| | FAHCLPSO [17] | 4.4877 | - |
| | SHADE-EC [36] | 4.8612 | 0.9205 |
| | DE [37] | 4.5550 | 1.9589 |
| | OGSA [38] | 4.4984 | 0.8085 |
| | HFA [39] | 4.529 | 1.625 |
| 2 | CEO | 5.4939 | 0.0874 |
| | EO | 5.1544 | 0.0915 |
| | MFO [10] | - | 0.12154 |
| | IGSA-CSS [12] | - | 0.08968 |
| | SHADE-EC [36] | 5.4495 | 0.08886 |
| | HFA [39] | 5.75 | 0.0980 |
| 3 | CEO | 4.8779 | 0.0998 |
| | EO | 4.8777 | 0.1038 |

According to the result in 3 cases, CEO is marginally way better than EO, 4.4107, 0.0874, 5.8764 MW compares to 4.4197, 0.0915, 5.9152 MW, respectively. Furthermore, the VD is littler for CEO, demonstrating improved voltage profile. Table 2 presents a comparison of CEO and EO against other optimization methods such as MFO, QOTLBO, IGSA-CSS, and different others. CEO yields a lowest power loss, making it one of the foremost effective methods in terms of lessening dynamic control misfortune. When comparing with other strategies, CEO shows superior in general framework voltage steadiness.

Figures 3 and 4 show the merging CEO and EO characteristics for Cases 1 and 2. CEO reliably illustrates quicker merging than EO, especially within the early stages of the optimization prepare. In Figure 3, CEO comes to a near-optimal wellness esteem of around 4.41 inside 100 cycles, whereas EO requires nearly 300 cycles to realize the same wellness esteem. Besides, CEO keeps up lower wellness work values all through the optimization handle. In Figure 4, CEO achieves speedier merging with a wellness work near to 0.1 in fair beneath 100 emphases, while EO slacks somewhat behind, requiring more cycles to reach a comparative level of optimization.

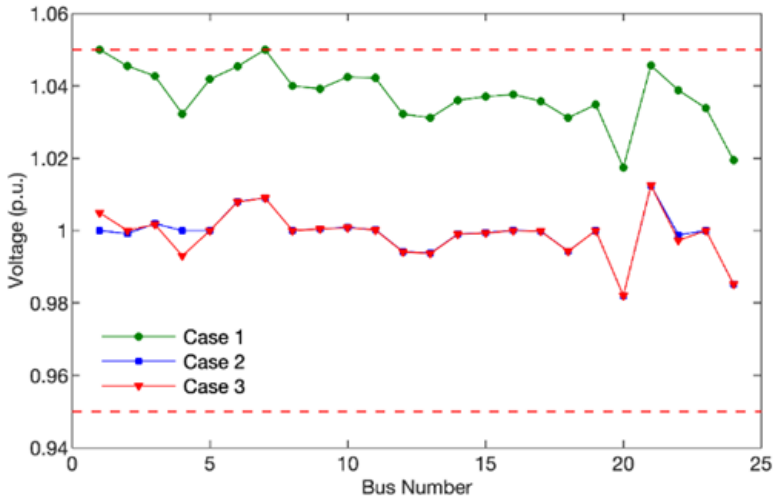


Figure 2. The load bus voltage of system for Cases 1, 2, and 3 of the conventional ORPD problem

These joining comes about highlight CEO's advantage in both the speed of finding ideal arrangements and keeping up superior wellness values all through the method, making it a more viable strategy for large-scale control framework optimization issues like ORPD. CEO gives lower control

misfortunes over all cases compared to EO and most other strategies. Usually pivotal for progressing the generally proficiency of control frameworks. CEO too accomplishes way better voltage solidness, as prove by the lower voltage deviation values in each case. The speedier merging of CEO, as appeared within the wellness work plots, shows that it can discover ideal arrangements more rapidly, making it computationally proficient for real-time applications.

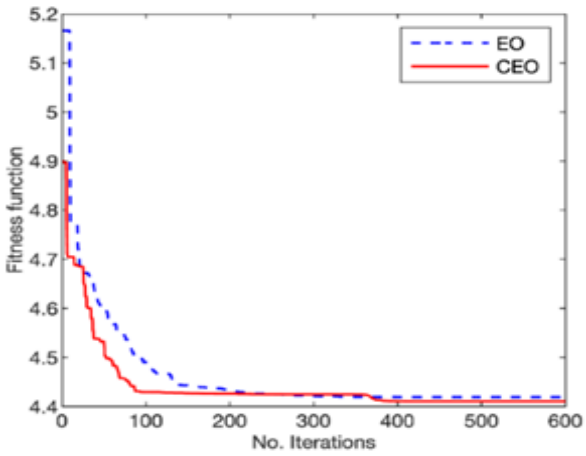


Figure 3. The convergence characteristics of the EO and CEO methods of the conventional ORPD problem for Case 1

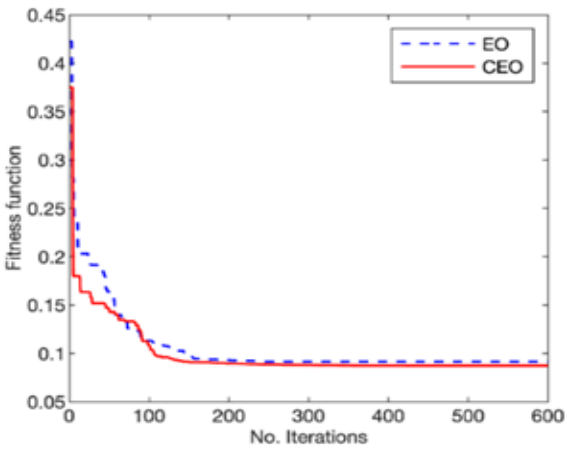


Figure 4. The convergence characteristics of the EO and CEO methods of the conventional ORPD problem for Case 2

### 3.1.2. The case of multi-objective function

The CEO method is implemented to solve the ORPD issue with combined objectives of active power loss and *VD* to test the efficiency of the suggested CEO in resolving the ORPD with multi-objective functions. Table 1 lists the most suitable settings of control variables and the best fitness function value obtained by the CEO and EO for this case. From the results, CEO yields a better fitness function value than the EO method. Moreover, the dependent variables stay in their predefined limitations, as shown in Table 1 and Figure 2. The real power loss and *VD* obtained by the proposed CEO are also compared to those from the CE method in Table 2. The comparison of results has shown that the real power loss from the both methods are the same but the *VD* value from the CEO method is better than that of the CE. Figure 5 also illustrates the proposed CEO and EO's convergence characteristics of for Case 3 concerning the ORPD problem. According to the graph, CEO exhibits superior convergence characteristics compared to EO. Therefore, CEO outperforms EO in both convergence speed and solution quality in Case 3.

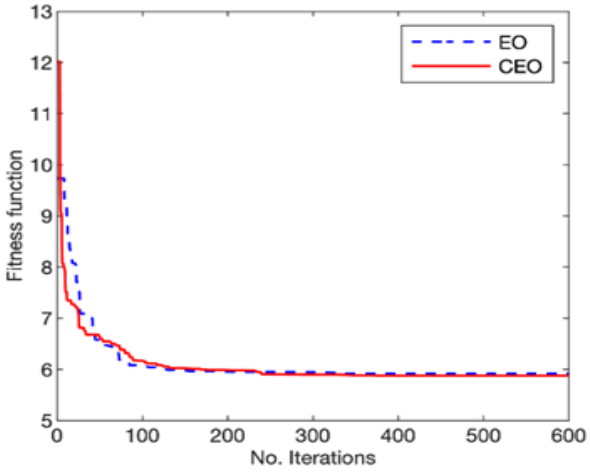


Figure 5. The convergence characteristics of the EO and CEO methods for Case 3 of the conventional ORPD problem

### 3.2. The TDORPD problem

When considering the temperature impact on resistance of branches, the TDORPD problem is considered with two case studies including Case 1 for the single-objective function and Case 2 for the multi-objective function. For the TDORPD issue in this case of study, the chosen base temperature ($T_{Base}$) is 100 °C. The reference temperature ($T_{Ref}$) and ambient temperature ($T_{Amp}$) are all chosen as 25 °C.

#### 3.2.1. The case of singe-objective function

With the single-objective function in Case 1, the active power loss in branches is selected as the objective function to be optimized. Table 3 and Figure 6 show the obtained active power loss by the TDORPD problem according to the changes in temperature. As observed from Table 3, the active power loss at 0°C from the proposed method was 4.4111 MW, which is increased to 4.5964 MW corresponding to a temperature rise of 100 °C. Thus, it can be inferred that the active power loss in the system raises with the temperature rise. Actually, the increment in active power loss is 0.42% corresponding to every 10 °C.

The results obtained by the proposed CEO for the test system are also compared to those from the EO for the TDORPD problem, as presented in Table 3. Across all considered temperature rises, the proposed CEO consistently yields superior solutions compared to other methods. Specifically, at the 30 °C rise of temperature, the proposed method achieves a 4.4781 MW active power loss, which is smaller than the 4.4844 MW obtained by the EO. Additionally, Table 4 provides details on the control configuration and fitness function results obtained by the proposed CEO for Case 1 at 30 °C. Furthermore, Figure 7 illustrates the convergence curves of both EO and CEO methods in Case 1 with a 30 °C temperature rise, demonstrating that the proposed method exhibits better convergence characteristics than the EO method.

Table 3. Result comparison of the obtained results from the CEO and EO methods for Case 1 of the TDORPD problem

| $T_{RatedRise}$ | Active power loss (MW) | |
|---|---|---|
| | CEO | EO |
| 0 | 4.4111 | 4.4204 |
| 10 | 4.4345 | 4.4401 |
| 20 | 4.4570 | 4.4606 |
| 30 | 4.4781 | 4.4844 |
| 40 | 4.4977 | 4.5028 |
| 50 | 4.5184 | 4.5203 |
| 60 | 4.5345 | 4.5434 |
| 70 | 4.5516 | 4.5614 |
| 80 | 4.5668 | 4.5713 |
| 90 | 4.5818 | 4.5934 |
| 100 | 4.5964 | 4.6009 |

Table 4. Optimal results for Case 1 and Case 2 of the TDORPD problem at 30 °C

| Parameters | Case 1 | | Case 2 | |
|---|---|---|---|---|
| | CEO | EO | CEO | EO |
| $V_{G1}$ (pu) | 1.0691 | 1.0671 | 1.0278 | 1.0279 |
| $V_{G2}$ (pu) | 1.0605 | 1.0583 | 1.0196 | 1.0203 |
| $V_{G5}$ (pu) | 1.0367 | 1.0345 | 1.0019 | 1.0026 |
| $V_{G8}$ (pu) | 1.0426 | 1.0401 | 1.0040 | 1.0052 |
| $V_{G11}$ (pu) | 1.0931 | 1.0712 | 1.0753 | 1.0448 |
| $V_{G13}$ (pu) | 1.0546 | 1.0675 | 0.9929 | 1.0018 |
| $Q_{C10}$ (MVar) | 0.7431 | 4.8539 | 4.9975 | 4.9992 |
| $Q_{C12}$ (MVar) | 0.0543 | 0.0466 | 0.0023 | 0.0969 |
| $Q_{C15}$ (MVar) | 4.0415 | 4.8520 | 4.9996 | 4.9979 |
| $Q_{C17}$ (MVar) | 4.9998 | 4.9997 | 0.0073 | 0.2750 |
| $Q_{C20}$ (MVar) | 3.9748 | 3.8531 | 5.0000 | 4.9905 |
| $Q_{C21}$ (MVar) | 4.9997 | 4.9785 | 4.9998 | 4.9959 |
| $Q_{C23}$ (MVar) | 2.9670 | 2.5918 | 4.9995 | 4.9999 |
| $Q_{C24}$ (MVar) | 5.0000 | 4.9999 | 4.9996 | 4.9972 |
| $Q_{C29}$ (MVar) | 2.3744 | 2.4541 | 2.5983 | 2.6631 |
| $T_{11}$ (pu) | 1.0486 | 1.0013 | 1.1000 | 1.0638 |
| $T_{12}$ (pu) | 0.9393 | 0.9832 | 0.9000 | 0.9004 |
| $T_{15}$ (pu) | 0.9859 | 1.0094 | 0.9504 | 0.9672 |
| $T_{36}$ (pu) | 0.9755 | 0.9743 | 0.9663 | 0.9664 |
| Active power loss (MW) | 4.4781 | 4.4844 | 4.9566 | 4.9382 |
| *VD* (p.u.) | 0.9061 | 0.9036 | 0.1017 | 0.1049 |
| Fitness function value | 4.4781 | 4.4844 | 5.9738 | 5.9873 |

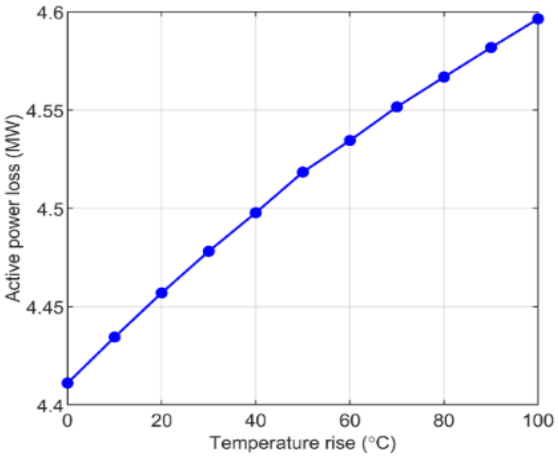


Figure 6. Temperature effect on active power loss for Case 1 of TDORPD problem

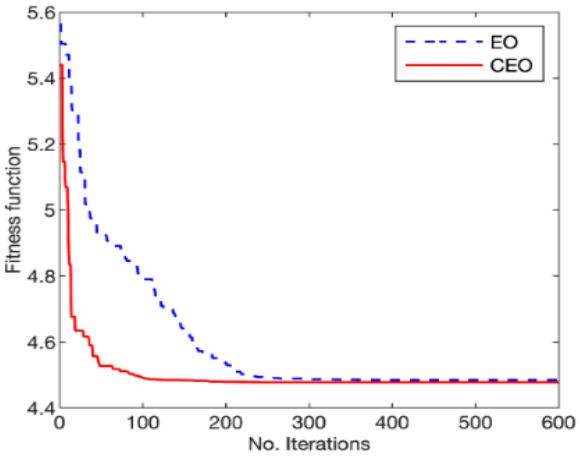


Figure 7. The convergence characteristics of both EO and CEO methods for Case 1 at 30 °C

### 3.2.2. The case of multi-objective function

The active power loss and voltage deviation are simultaneously examined as a multi-objective function of the TDORPD problem in this scenario. Table 5 showcases the optimum results attained by the proposed EO and CEO methods for this particular problem. Considering a temperature at 0 °C, the proposed CEO achieves an active power loss of 4.8776 MW and a voltage deviation of 0.1 p.u., yielding a fitness value of 5.8781 as per (12). As the temperature rise escalates to 100 °C, the proposed CEO delivers an active power loss, voltage deviation, and calculated fitness value of 5.0942 MW, 0.1059 p.u., and 6.1534, respectively. Additionally, the impact of the temperature rises on the fitness function value for Case 2 utilizing the proposed CEO is illustrated in Figure 8, revealing a tendency for the fitness function result to rise accordingly to the temperature increasing.

For a 10 °C temperature increment, there is an estimated 0.47% increase in the value of the fitness function when employing the suggested CEO algorithm. Featuring a temperature at 30 °C, Table 4 outlines the optimum outputs obtained by the CEO approach for Case 2. Contrastingly, when compared to Case 1 with the similar temperature rise, the voltage deviation enhances from 0.9061 p.u. to 0.1017 p.u., while the active power loss increases from 4.4781 MW to 4.9566 MW. Additionally, Figure 9 shows the convergence characteristic of the proposed EO and CEO methods for Case 2 at 30°C. It can be seen from Figure 9 where the CEO's fitness function converges after 400 iterations, which is superior to the EO method.

Table 5. Result comparison of the proposed CEO and EO methods for Case 2 of the TDORPD problem

| $T_{RatedRise}$ | EO | | | CEO | | |
|---|---|---|---|---|---|---|
| | Fitness function | Power loss (MW) | *VD* (p.u.) | Fitness function | Power loss (MW) | *VD* (p.u.) |
| 0 | 5.8887 | 4.8606 | 0.1028 | 5.8781 | 4.8776 | 0.1000 |
| 10 | 5.9210 | 4.8894 | 0.1032 | 5.9124 | 4.9064 | 0.1006 |
| 20 | 5.9638 | 4.9236 | 0.1040 | 5.9439 | 4.9370 | 0.1007 |
| 30 | 5.9873 | 4.9382 | 0.1049 | 5.9738 | 4.9566 | 0.1017 |
| 40 | 6.0226 | 4.9718 | 0.1051 | 6.0056 | 4.9825 | 0.1023 |
| 50 | 6.0404 | 5.0102 | 0.1030 | 6.0301 | 5.0150 | 0.1015 |
| 60 | 6.0807 | 5.0113 | 0.1069 | 6.0597 | 5.0243 | 0.1035 |
| 70 | 6.0881 | 5.0327 | 0.1055 | 6.0826 | 5.0398 | 0.1043 |
| 80 | 6.1100 | 5.0640 | 0.1046 | 6.1097 | 5.0574 | 0.1052 |
| 90 | 6.1401 | 5.0513 | 0.1089 | 6.1359 | 5.0501 | 0.1086 |
| 100 | 6.1699 | 5.0789 | 0.1091 | 6.1534 | 5.0942 | 0.1059 |

Figures 8 and 9 provide additional information on the performance of the two methods. Figure 8 shows the increasing temperature effect on the fitness function result in Case 2, where the fitness function for both methods increase with increasing temperature. The CEO method consistently achieves lower fitness function values than the EO method, reflecting better overall optimization performance. For example, at 0 °C, the CEO method achieves the fitness function value of 5.8781, while it is 5.8887 for the EO method. At 100 °C, these values increase to 6.1534 for CEO and 6.1699 for EO, maintaining a similar performance gap. The convergence characteristics of the EO and CEO methods in Figure 9 are illustrated at 30 °C. Both

methods converge as the number of iterations increases, but the CEO method converges faster and achieves a lower fitness function value than the EO. This shows that the CEO method not only provides better optimization in terms of power loss and VD but also exhibits superior convergence behavior, which is essential for computational efficiency in solving large-scale optimization problems. Overall, the CEO method continues to outperform the EO method in terms of minimizing power loss, voltage deviation, and fitness function values, and achieving more consistent rapid convergence in the TDORPD problem. These benefits make CEO a more effective choice for solving complex power system optimization challenges, especially when considering environmental variables such as temperature rise.

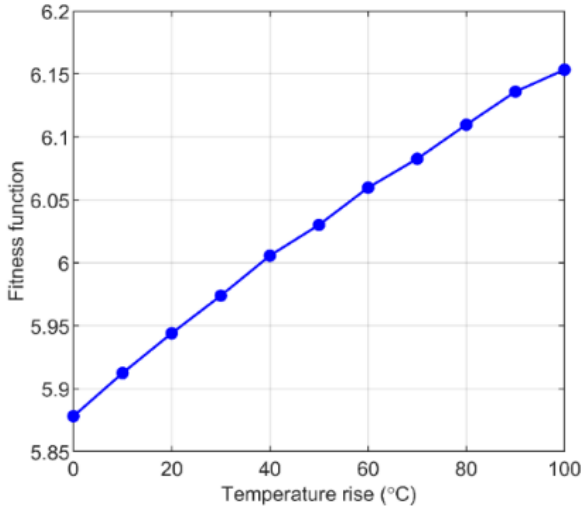


Figure 8. The effects of temperature on the fitness function in Case 2 of the TDORPD problem

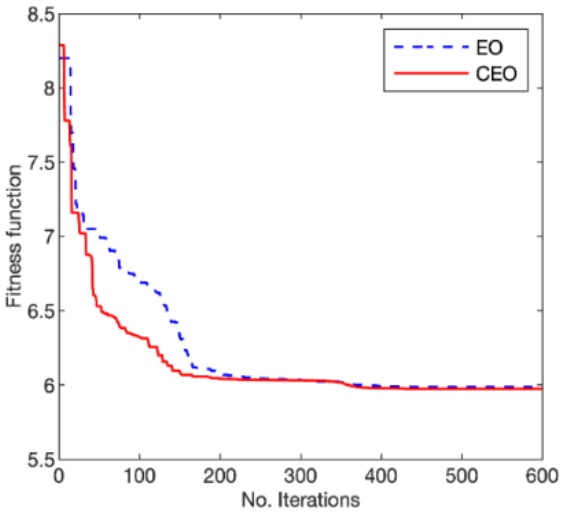


Figure 9. The convergence characteristics of the proposed EO and CEO methods in Case 2 of the TDORPD problem at 30 ℃

## 4. CONCLUSION

In this paper, the TDORPD problem has been successfully solved by a new CEO method considering the effect of temperature on the power flow problems. The proposed method was developed by integrating the chaotic local search to boost its search ability. Both the objective functions of active power loss and voltage deviation were taken into account in different case studies for the both conventional ORPD and TDORPD problems. The efficacy of the suggested CEO is tested on the IEEE 30-bus network with different temperature rises. In practice, it is evident that fluctuations in temperature directly impact the fitness function value when solving the TDORPD problem. Therefore, by factoring in the temperature's influence, the precision of the power flow calculation in the TDORPD problem is significantly enhanced. From comparative results, the proposed CEO is capable of yield better quality solutions compared to the conventional EO method and other approaches. Therefore, the solutions quality, as well as the convergence characteristic of the proposed CEO has a great potential for future research on other power system optimization problems. The results of the TDORPD problem demonstrate that the CEO method consistently outperforms the EO method on key parameters such as power loss, VD, and the value of the fitness function. In Cases 1 and 2, OEB produces lower active power loss with increasing temperature, with a more favorable performance for minimizing VD. For example, in Case 2, at a temperature increase of 100 °C, OEB reaches a real power loss of 5.0942 MW in comparison to 5.0789 MW for EO, as well as lower VD values. Furthermore, the CEO method has a clear advantage in minimizing the fitness function, with systematically lower values than the EO method under all temperature conditions. This advantage is further emphasized by its faster convergence behavior, as shown in the respective convergence plots for both cases. Overall, the CEO method proves to be more efficient and effective in solving the TDORPD problem, making it a better choice for dealing with the complexity of power systems, especially under varying temperature conditions.

Future development of temperature-dependent ORPD using chaotic equilibrium optimization algorithms has significant potential to improve the performance and reliability of power systems. With its focus on real-time integration, scalability, adaptability to renewable energy, and robustness to uncertainties, this approach could play an irreplaceable role in the evolving landscape of smart grids and modern power

systems. Further research, development, and practical implementation will be necessary to realize its full potential.

## ACKNOWLEDGMENT

We acknowledge Ho Chi Minh City University of Technology (HCMUT), VNU-HCM for supporting this study.

## REFERENCES

[1] E. Rezania and S. M. Shahidehpour, "Real power loss minimization using interior point method," *International Journal of Electrical Power and Energy System*, vol. 23, no. 1, pp. 45–56, 2001, doi: 10.1016/S0142-0615(00)00028-4.
[2] J. Z. Zhu and X. F. Xiong, "Optimal reactive power control using modified interior point method," *Electric Power Systems Research*, vol. 66, no. 2, pp. 187–192, Aug. 2003, doi: 10.1016/S0378-7796(03)00078-6.
[3] R. Mota-Palomino and V. H. Quintana, "Sparse reactive power scheduling by a penalty function - linear programming technique," *IEEE Transactions on Power Systems*, vol. 1, no. 3, pp. 31–39, 1986, doi: 10.1109/TPWRS.1986.4334951.
[4] R. C. Burchett, H. H. Happ, and D. R. Vierath, "Quadratically convergent optimal power flow," *IEEE Transactions on Power Apparatus and Systems*, vol. PAS-103, no. 11, pp. 3267–3275, Nov. 1984, doi: 10.1109/TPAS.1984.318568.
[5] D. I. Sun, B. Ashley, B. Brewer, A. Hughes, and W. F. Tinney, "Optimal power flow by Newton approach," *IEEE Transactions on Power Apparatus and Systems*, vol. PAS-103, no. 10, pp. 2864–2880, Oct. 1984, doi: 10.1109/TPAS.1984.318284.
[6] O. Alsac and B. Stott, "Optimal load flow with steady-state security," *IEEE Transactions on Power Apparatus and Systems*, vol. PAS-93, no. 3, pp. 745–751, May 1974, doi: 10.1109/TPAS.1974.293972.
[7] N. Grudinin, "Reactive power optimization using successive quadratic programming method," *IEEE Transactions on Power Systems*, vol. 13, no. 4, pp. 1219–1225, 1998, doi: 10.1109/59.736232.
[8] F. C. Lu and Y. Y. Hsu, "Reactive power/voltage control in a distribution substation using dynamic programming," *IEE Proceedings: Generation, Transmission and Distribution*, vol. 142, no. 6, pp. 639–645, 1995, doi: 10.1049/ip-gtd:19952210.
[9] V. A. De Sousa, E. C. Baptista, and G. R. M. Da Costa, "Optimal reactive power flow via the modified barrier Lagrangian function approach," *Electric Power Systems Research*, vol. 84, no. 1, pp. 159–164, Mar. 2012, doi: 10.1016/j.epsr.2011.11.001.
[10] R. Ng Shin Mei, M. H. Sulaiman, Z. Mustaffa, and H. Daniyal, "Optimal reactive power dispatch solution by loss minimization using moth-flame optimization technique," *Applied Soft Computing Journal*, vol. 59, pp. 210–222, Oct. 2017, doi: 10.1016/j.asoc.2017.05.057.
[11] A. A. Heidari, R. Ali Abbaspour, and A. Rezaee Jordehi, "Gaussian bare-bones water cycle algorithm for optimal reactive power dispatch in electrical power systems," *Applied Soft Computing Journal*, vol. 57, pp. 657–671, Aug. 2017, doi: 10.1016/j.asoc.2017.04.048.
[12] G. Chen, L. Liu, Z. Zhang, and S. Huang, "Optimal reactive power dispatch by improved GSA-based algorithm with the novel strategies to handle constraints," *Applied Soft Computing*, vol. 50, pp. 58–70, Jan. 2017, doi: 10.1016/j.asoc.2016.11.008.
[13] B. Mandal and P. K. Roy, "Optimal reactive power dispatch using quasi-oppositional teaching learning based optimization," *International Journal of Electrical Power and Energy Systems*, vol. 53, no. 1, pp. 123–134, Dec. 2013, doi: 10.1016/j.ijepes.2013.04.011.
[14] Y. Li, X. Li, and Z. Li, "Reactive power optimization using hybrid CABC-DE algorithm," *Electric Power Components and Systems*, vol. 45, no. 9, pp. 980–989, May 2017, doi: 10.1080/15325008.2017.1311387.
[15] A. Rajan and T. Malakar, "Exchange market algorithm based optimum reactive power dispatch," *Applied Soft Computing Journal*, vol. 43, pp. 320–336, Jun. 2016, doi: 10.1016/j.asoc.2016.02.041.
[16] M. S. Alam and M. De, "Optimal reactive power dispatch using hybrid loop-genetic based algorithm," in *2016 National Power Systems Conference, NPSC 2016*, IEEE, Dec. 2016, pp. 1–6. doi: 10.1109/NPSC.2016.7858901.
[17] E. Naderi, H. Narimani, M. Fathi, and M. R. Narimani, "A novel fuzzy adaptive configuration of particle swarm optimization to solve large-scale optimal reactive power dispatch," *Applied Soft Computing Journal*, vol. 53, pp. 441–456, Apr. 2017, doi: 10.1016/j.asoc.2017.01.012.
[18] R. Muzzammel, R. Arshad, S. Bashir, U. Mushtaq, F. Durrani, and S. Noshin, "Comparative analysis of optimal power flow in renewable energy sources based microgrids," *International Journal of Electrical and Computer Engineering (IJECE)*, vol. 13, no. 2, pp. 1241–1259, Apr. 2023, doi: 10.11591/ijece.v13i2.pp1241-1259.
[19] K. Abaci and V. Yamaçli, "Optimal reactive-power dispatch using differential search algorithm," *Electrical Engineering*, vol. 99, no. 1, pp. 213–225, Mar. 2017, doi: 10.1007/s00202-016-0410-5.
[20] A. Mukherjee and V. Mukherjee, "Chaos embedded krill herd algorithm for optimal VAR dispatch problem of power system," *International Journal of Electrical Power and Energy Systems*, vol. 82, pp. 37–48, Nov. 2016, doi: 10.1016/j.ijepes.2016.02.039.
[21] M. H. Sulaiman, Z. Mustaffa, M. R. Mohamed, and O. Aliman, "Using the gray wolf optimizer for solving optimal reactive power dispatch problem," *Applied Soft Computing Journal*, vol. 32, pp. 286–292, Jul. 2015, doi: 10.1016/j.asoc.2015.03.041.
[22] S. Mouassa, T. Bouktir, and A. Salhi, "Ant lion optimizer for solving optimal reactive power dispatch problem in power systems," *Engineering Science and Technology, an International Journal*, vol. 20, no. 3, pp. 885–895, Jun. 2017, doi: 10.1016/j.jestch.2017.03.006.
[23] M. Balasubbareddy, D. Dwivedi, G. V. K. Murthy, and K. S. Kumar, "Optimal power flow solution with current injection model of generalized interline power flow controller using ameliorated ant lion optimization," *International Journal of Electrical and Computer Engineering (IJECE)*, vol. 13, no. 1, pp. 1060–1077, Feb. 2023, doi: 10.11591/ijece.v13i1.pp1060-1077.
[24] K. ben oualid Medani, S. Sayah, and A. Bekrar, "Whale optimization algorithm based optimal reactive power dispatch: A case study of the Algerian power system," *Electric Power Systems Research*, vol. 163, pp. 696–705, Oct. 2018, doi: 10.1016/j.epsr.2017.09.001.
[25] T. P. Naidu, G. Balasubramanian, and B. V. Rao, "Optimal power flow with distributed energy sources using whale optimization algorithm," *International Journal of Electrical and Computer Engineering (IJECE)*, vol. 13, no. 5, pp. 4835–4844, Oct. 2023, doi: 10.11591/ijece.v13i5.pp4835-4844.
[26] V. Alagapuri, A. B. Radhakrishnan, S. Sithangkathan, and J. Kalikrishnan, "Optimization of location and rating of unified power flow controllers for congestion management," *Indonesian Journal of Electrical Engineering and Computer Science (IJEECS)*, vol. 29, no. 3, pp. 1258–1267, Mar. 2023, doi: 10.11591/ijeecs.v29.i3.pp1258-1267.

[27] A. M. Shaheen, R. A. El-Sehiemy, and S. M. Farrag, "Optimal reactive power dispatch using backtracking search algorithm," *Australian Journal of Electrical and Electronics Engineering*, vol. 13, no. 3, pp. 200–210, Jul. 2016, doi: 10.1080/1448837X.2017.1325134.
[28] T. T. Nguyen, D. N. Vo, H. Van Tran, and L. Van Dai, "Optimal dispatch of reactive power using modified stochastic fractal search algorithm," *Complexity*, vol. 2019, no. 1, Jan. 2019, doi: 10.1155/2019/4670820.
[29] T. T. Nguyen and D. N. Vo, "Improved social spider optimization algorithm for optimal reactive power dispatch problem with different objectives," *Neural Computing and Applications*, vol. 32, no. 10, pp. 5919–5950, May 2020, doi: 10.1007/s00521-019-04073-4.
[30] M. H. Ali, A. M. A. Soliman, and S. K. Elsayed, "Optimal power flow using archimedes optimizer algorithm," *International Journal of Power Electronics and Drive Systems (IJPEDS)*, vol. 13, no. 3, pp. 1390–1405, Sep. 2022, doi: 10.11591/ijpeds.v13.i3.pp1390-1405.
[31] S. Frank, J. Sexauer, and S. Mohagheghi, "Temperature-dependent power flow," *IEEE Transactions on Power Systems*, vol. 28, no. 4, pp. 4007–4018, Nov. 2013, doi: 10.1109/TPWRS.2013.2266409.
[32] M. Basu, "Quasi-oppositional differential evolution for optimal reactive power dispatch," *International Journal of Electrical Power and Energy Systems*, vol. 78, pp. 29–40, Jun. 2016, doi: 10.1016/j.ijepes.2015.11.067.
[33] A. Faramarzi, M. Heidarinejad, B. Stephens, and S. Mirjalili, "Equilibrium optimizer: A novel optimization algorithm," *Knowledge-Based Systems*, vol. 191, p. 105190, Mar. 2020, doi: 10.1016/j.knosys.2019.105190.
[34] S. Mirjalili, S. M. Mirjalili, and A. Lewis, "Grey Wolf Optimizer," *Advances in Engineering Software*, vol. 69, pp. 46–61, Mar. 2014, doi: 10.1016/j.advengsoft.2013.12.007.
[35] M. Aljebreen, M. Obayya, H. Mahgoub, S. S. Alotaibi, A. Mohamed, and M. A. Hamza, "Chaotic equilibrium optimizer-based green communication with deep learning enabled load prediction in internet of things environment," *IEEE Access*, vol. 12, pp. 258–267, 2024, doi: 10.1109/ACCESS.2023.3345803.
[36] P. P. Biswas, P. N. Suganthan, R. Mallipeddi, and G. A. J. Amaratunga, "Optimal reactive power dispatch with uncertainties in load demand and renewable energy sources adopting scenario-based approach," *Applied Soft Computing Journal*, vol. 75, pp. 616–632, Feb. 2019, doi: 10.1016/j.asoc.2018.11.042.
[37] A. A. A. El Ela, M. A. Abido, and S. R. Spea, "Differential evolution algorithm for optimal reactive power dispatch," *Electric Power Systems Research*, vol. 81, no. 2, pp. 458–464, Feb. 2011, doi: 10.1016/j.epsr.2010.10.005.
[38] B. Shaw, V. Mukherjee, and S. P. Ghoshal, "Solution of reactive power dispatch of power systems by an opposition-based gravitational search algorithm," *International Journal of Electrical Power and Energy Systems*, vol. 55, pp. 29–40, Feb. 2014, doi: 10.1016/j.ijepes.2013.08.010.
[39] A. Rajan and T. Malakar, "Optimal reactive power dispatch using hybrid Nelder-Mead simplex based firefly algorithm," *International Journal of Electrical Power and Energy Systems*, vol. 66, pp. 9–24, Mar. 2015, doi: 10.1016/j.ijepes.2014.10.041.

## BIOGRAPHIES OF AUTHORS

**Minh Trung Dao** received a B.Sc. degree in Electrical Engineering from Can Tho University, Vietnam, in 2005 and M.Eng. degree in Electrical Engineering from University of Technology-Viet Nam National University Ho Chi Minh City in 2012. Since 2005, he has been with the Department of Electrical Engineering, Can Tho University in Can Tho city, Viet Nam, where he is currently a lecturer. His research interests include power system optimization, power system operation and control, power system analysis, and renewable energy systems. Now, he is also a Ph.D. student at University of Technology-Viet Nam National University Ho Chi Minh City (from 8/2021). He can be contacted at email: dmtrung.sdh21@hcmut.edu.vn.

**Ngoc Dieu Vo** received his B.Eng. and M.Eng. degrees in electrical engineering from Ho Chi Minh City University of Technology, Ho Chi Minh city, Vietnam, in 1995 and 2000, respectively and his D.Eng. degree in energy from Asian Institute of Technology (AIT), Pathumthani, Thailand in 2007. He is Research Associate at Energy Field of Study, AIT and Head of Department of Power Systems, Faculty of Electrical and Electronic Engineering, Ho Chi Minh City University of Technology, Ho Chi Minh city, Vietnam. His research interests are applications of AI in power system optimization, power system operation and control, power system analysis, and power systems under deregulation and restructuring. He can be contacted at email: vndieu@hcmut.edu.vn.